Egyptian Journal of Geology, v. 63, 2019, p. 133-149

GEOCHEMICAL INVESTIGATION OF THE MIDDLE AND THE UPPER JURASSIC ROCKS, WELL HF35/1, ABU SENNAN AREA, NORTH WESTERN DESERT, EGYPT

Attia, G. M. [1], Edress, N. A. A. [1], and Mahmoud, A. A. [1]

[1]Helwan University, Faculty of Science, Geology Department.

ABSTRACT

The Abu Sennan area is located at the southern rim of the Abu Gharadig basin east of Qattara topographic depression. The whole lithostratigraphic units throughout the well HF35/1 of the study area are mentioned in the present study. The deepest sedimentary succession of both the Middle Jurassic (Khatatba Fm.) and the Upper Jurassic (Masajid Fm.) was chosen to evaluate their capability for hydrocarbon production and their sedimentary setting in the studied well. Twenty-seven cutting samples from the present Formations were subjected to organic geochemical analysis using Rock-Eval pyrolysis technique. A twenty-four samples represented the Middle Jurassic and three samples of the Upper Jurassic were examined. The TOC values of the present succession reveal that the Masajid Formation has extremely fair quantity (average; 0.52 wt%), whereas the Khatatba Formation contains favorable hydrocarbon of good to very good quantity (average; 1.53 wt, %). However, the freely released hydrocarbons during pyrolysis indicates the domain of poor and fair petroleum potential for both formations. The plotting samples of the studied formations on the production yield (Py) versus TOC diagram confirms that the Masajid Formation is poor where the Khtatba Formation is dominant of fair petroleum potential. The kerogen type of the Masajid is Type III of hydrogen index (HI) values between 60.38 and 76 (mg HC/g TOC) and an S2/S3 ratio is around 3. The Khatatba is the same as the Masajid of the majority of type III with a little sample of type II/III did not exceed 12 % of the total examined samples. The latter type II/III represents the lowermost part of the Khatatba Formation. The dominance of kerogen III in the studied formations may relate to the proximity of sedimentation processes to the shore of the basin and/or the flourish of the terrestrial land plant during this period. The maturity parameters of Tmax, PI (production index), and Ro (vitrinite reflectance) of the studied formations show a late stage of maturity within a condensate wet gas (gas window) of the low conversion. Statistical analysis of the studied samples shows that the mature zone is considered to be within depth intervals of 2700m to 4150m.

Keywords: Organic geochemistry, lithostratigraphic Units, Vitrinite reflectance, Jurassic rocks, Abu Sennan area

INTRODUCTION

The Abu Sennan area is occupied the eastern area of the topographic depression of the Qatara in the North Western Desert. It locates between latitudes of 29°33` and 29°22` N and longitudes 28°22` and 28°37` E. It represents the southern rim of the main important hydrocarbons basin of the Abu Gharadig in the Western Desert. A deepest drilled well (HF35/1) in the area was selected for this study to carry out stratigraphic and geochemical analysis. It has coordinates of latitude 29^0 30' 5" N and longitude $28^0$33' 9.5" E. The well was drilled in the 21 century upon the exploration activity by the General Petroleum Company in Abu Sennan area (Fig. 1). The investigated site included two concessions operated by General Petroleum Company (GPC) and NAFTOGAS Company while the most southern part is an abandonment area. The lithostratigraphic units within the area are as similar to those characterized the unstable shelf of the Egyptian territories. Lithostratigraphically, the column of the overlying series may be subdivided into three sequences: a, the "lower clastic unit", from Cambrian to Cenomanian; b, the "middle carbonates" from Turonian to Eocene; and c, the "upper clastic unit", from Oligocene to Recent (WEC, 1984).

Fig. 1: Location map of the studied well HF35/1, Abu Sennan, Western Desert.

The Western Desert has enormous hydrocarbon potential and many promising areas, such as the Abu Sennan area, await detailed examination. Many promising areas await detailed examination and are virtually untested by drilling. In 2010 GPC announced the positive discovery, namely HF35/1x. More than 15 development wells drilled in the Abu Sennan area. All the drilled wells turned as oil and gas producers from Abu Roash "C", "D", "E" and "G" Members. Based on the mentioned exploration discoveries, the upper Cretaceous Bahariya and Abu Roash Formations are qualified for hydrocarbon generation and oil entrapment in the study area. Dolson et al. (2014) mentioned that the only source rocks that are thermally mature are Ras Qattara, Khatatba, Alam El Buieb and Abu Roash Formations in the Western Desert (Fig. 2).

Accordingly, the main purpose of the present study is to give an idea of stratigraphic units and applying the organic geochemistry to evaluate the petroleum potentiality of the organic-rich formations of the upper part of Masajid and Khatatba of the Upper and Middle Jurassic in the well HF35/1 in the area of Abu Sennan from the viewpoint of petroleum system.

GEOLOGICAL SETTING

Structure geology

The Abu Sennan area is situated south of the Abu Gharadig basin. Abu Gharadig basin is a rift basin surrounded to the north and south by two right-lateral shears (Awad, 2008). It is a deep E-W trending asymmetric graben, with basement at depths over 10500 m. The structural pattern of Abu Gharadig Basin is dominated by NE-SW oriented faults coupled with a strong pattern of NW–SE conjugate faults. Three different types of faults affected Abu Gharadig basin, which is normal, reverse and strike-slip (right and left-lateral) faults. The most prime faults were initiated as simple tensional normal faults, trending mainly E-W, ENE, and WNW, but then developed a strong right lateral component (Awad, 2008). The major folds owe their origin to wrenching process compression movements, which affected the area during the Late Cretaceous-Early Tertiary tectonic events (RRI, 1982). As well as unconformities are present at various stratigraphic levels. Awad (2008) delineated a number of unconformities which are known through the Paleozoic; they are consequences of Early Paleozoic Caledonian and Late Paleozoic Hercynian tectonic events, which caused the north-south folding and block faulting system.

During the Late Cretaceous, The Abu Sennan area is affected by the main structure by the wrenching tectonics of the Syrian-Arc system (Bosworth, 2008; Salim et al., 2016) equivalent to the North Africa and the rest of Egypt. The compression features of folding and thrusting are clearly reflected in the structural pattern in most fields in an east Abu Sennan area (Salim et al., 2016). According to the Syrian-Arc

tectonic model, the folding and thrusting in the ENE-direction is associated with E-W to WNW-trending transtensional faulting and NW-trending extensional faults (Sehim, 1993; Moustafa et al., 1998). Salim et al., 2016 reported that main structures in the Abu Sennan area are found represented on the shallow level of Abu Roash Formation by dominant extensional faulting along the NW-direction with few WNW to E-W trending faulting. The latter faults were found more dominant with depth on the expense of the NW-trending faults. Changing fault style with depth can induce additional faulting in the walls of the main faults. Abu Sennan area, reflecting en echelon folds obeys the NE Syrian arc trend bonded by mid-basin, low in the North and Abu Sennan low in the South. Those two structural lows subjected to contain the major source rock which feeding the different culminations.

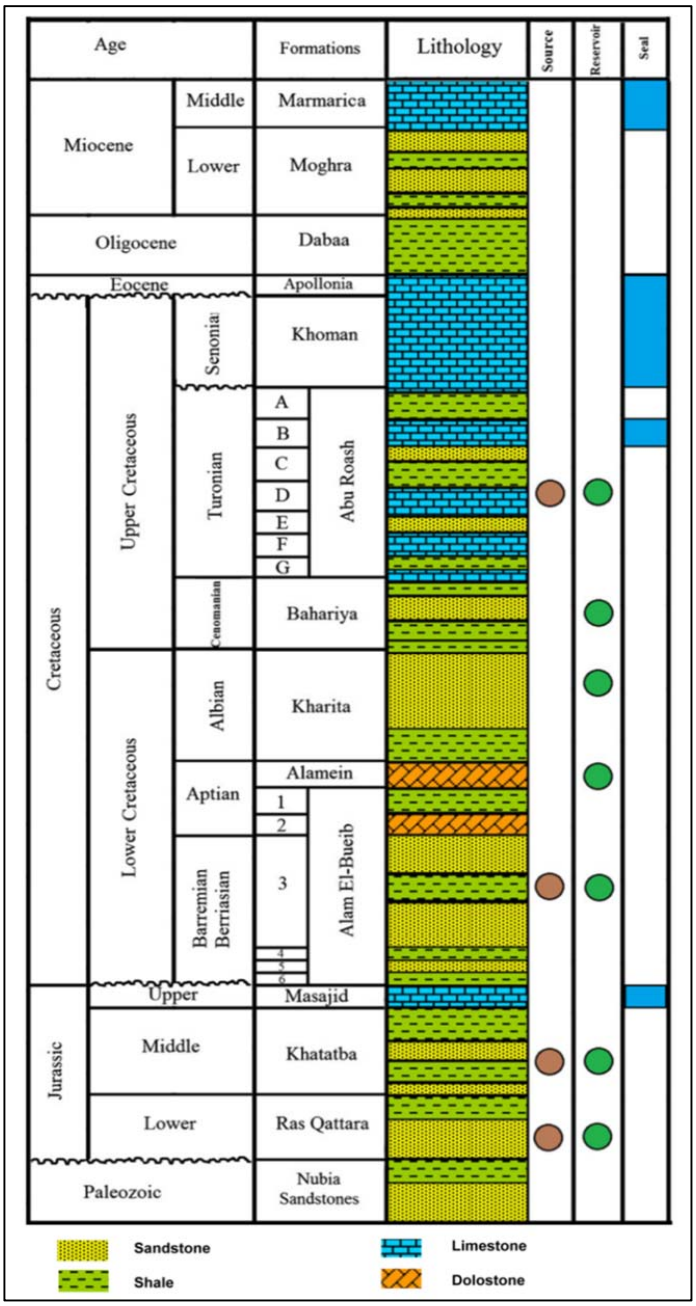

Fig. 2: General Stratigraphic succession of north Western Desert (Schlumberger 1995; Shalaby et al., 2012; and Dolson et al., 2014).

The Abu Gharadig basin is subdivided into several structural units of varying importance named from E to W: the Mubarak High, the Abu Gharadig Anticline and the Mid Basin Arch (Meshref 1990). Sehim (1993) reported that Cretaceous master wrenches are oriented in E-W to ENE directions. They signal a rejuvenation of inherited shear zones in the crystalline Precambrian rocks. The latter shears were

developed during the Pan African tectonic-thermal orogeny (Abdel Khalek et al. 1989). The first considerable rejuvenation of these Late Proterozoic shears was during the Early Mesozoic, concurrent with the opening of the Neo-Tethys.

The geologic evidence sheds a light on the extensional regime prevailing in Egypt during the opening of the Neo-Tethys in Triassic-Jurassic time. The extensional strain trajectories are suggested to be oriented principally around the N-S directions, and subordinately around E-W directions. Sets of basins with piles of sediments are lived to have initiated by such E-W extension.

Stratigraphy

The studied well HF35/1 is drilled by the combination of the GPC and NAFTOGAS companies in 1993. It is situated at latitudes 29^0 32' 08" N and longitude 28^0 29' 31" E with total depth 3916m. This well is pentrated strata belonging to Tertiary and Mesozoic times. The lithological interpretation of the stratigraphic successions penetrated in HF35/1, the lithological characteristics, the stratigraphical succession of the different formations and the depth of the drilled units are illustrated in (Fig. 3). Nine formations, which are encountered in this well. The lowermost Formations of the Upper Jurassic (Masajid) and Middle Jurassic (Khatatba) are described in descending stratigraphic order as follows:

Masajid Formation (Middle-Late Jurassic, Bathonian - Kimmeridgian): The Masajid Formation, in the present well is made up of marine massive limestones sequence and shales. The carbonate sequence is cherty in different parts. It overlies conformably the clastic Khatatba Formation and underlies unconformably the clastic lower Cretaceous sequence. In Abu Sennan area, the Masajid Formation was penetrated in HF35/1 well, at drill depth 3487 m to 3587 m (100 m thick). In Wadi El Natrun-1 well, Upper Jurassic sediments are predominantly clastics and include an abundance of reef-forming foraminiferal species. The Masajid Formation is of shallow marine origin deposited under relatively low energy environment (Hantar, 1990).

Khatatba Formation (Middle Jurassic, Bathonian-Early Callovian): Norton (1967) proposed the Khatatba Formation for a unit composed of dark gray shales, coaly shales, fine- to medium-grained sandstones, and a few shallow marine limestone beds. The type section is in the Khatatba-1 well, in the interval 355 m to 1536 m. The unit rests conformably on the Wadi Natrun Formation (Fig. 2) and is conformably overlain by the Masajid Formation (Tawadros, 2001; 2012). Khatatba Formation consists of a thick shallow marine carbonaceous shale sequence, with interbedded porous sandstone, oil-bearing in the Razzak field, coal seams and limestone streaks (El Shaarawy, 1994 a), with limited gas potential (Fawzy and Dahi, 1992).

The Khatatba Formation in the study area overlies the Yakout red shale and volcanic ashes which shown at the adjacent AGENS-1 well to the south (Attia et al., 2017), which characterize the top sequence of the earlier first Mesozoic rifting phase and the associating volcanic activity (Abdel Gawad, 2015; Sehim, 1993). Khatatba Formation was penetrated in HF35/1 well at drill depth 3587m to 3917 m (330 m thick).

SAMPLES AND METHODS

Twenty-seven cutting samples are selected and prepared for geochemical investigation. Only carbonaceous rich siliciclastics shale, siltstone and coaly shale sediments within each formation are selected at nearly the same intervals depths to examine. Moisture is removed from the samples by putting them in an oven of 40^o C for an hour**.** Approximately 200 mg of each sample is pulverized to 100 mesh by agate mortar. After that**,** the crushed samples are treated by HCL at 70^o C for carbonate removal. By combustion technique using LECO SC 632 instrument at the 1350 ^{o}C in the furnace of oxygen gas, the TOC of each sample was determined (Schumacher, 2002).

Another 65 mg of each bulk sample was analyzed by the Rock-Eval v6 instrument in the geochemical laboratory of the Egyptian Petroleum Research Institute. There are two values were obtained; the measured parameters and the calculated parameters. The measured parameters are: S1, freely volatile OM release when rock reach to 300^o C (mg HC/g rock); S2, the hydrocarbon generates by crackimg of solid

OM within temperature ranges of 300-600^{o} C; S3, the amount of the carbon dioxide that produced by the pyrolysis of OM (mg CO2/g rock); Tmax, the peak temperature of the pyrolysis maximum yield hydrocarbon of S2 (Tissot and Welte 1984; Espitalie et al 1997).

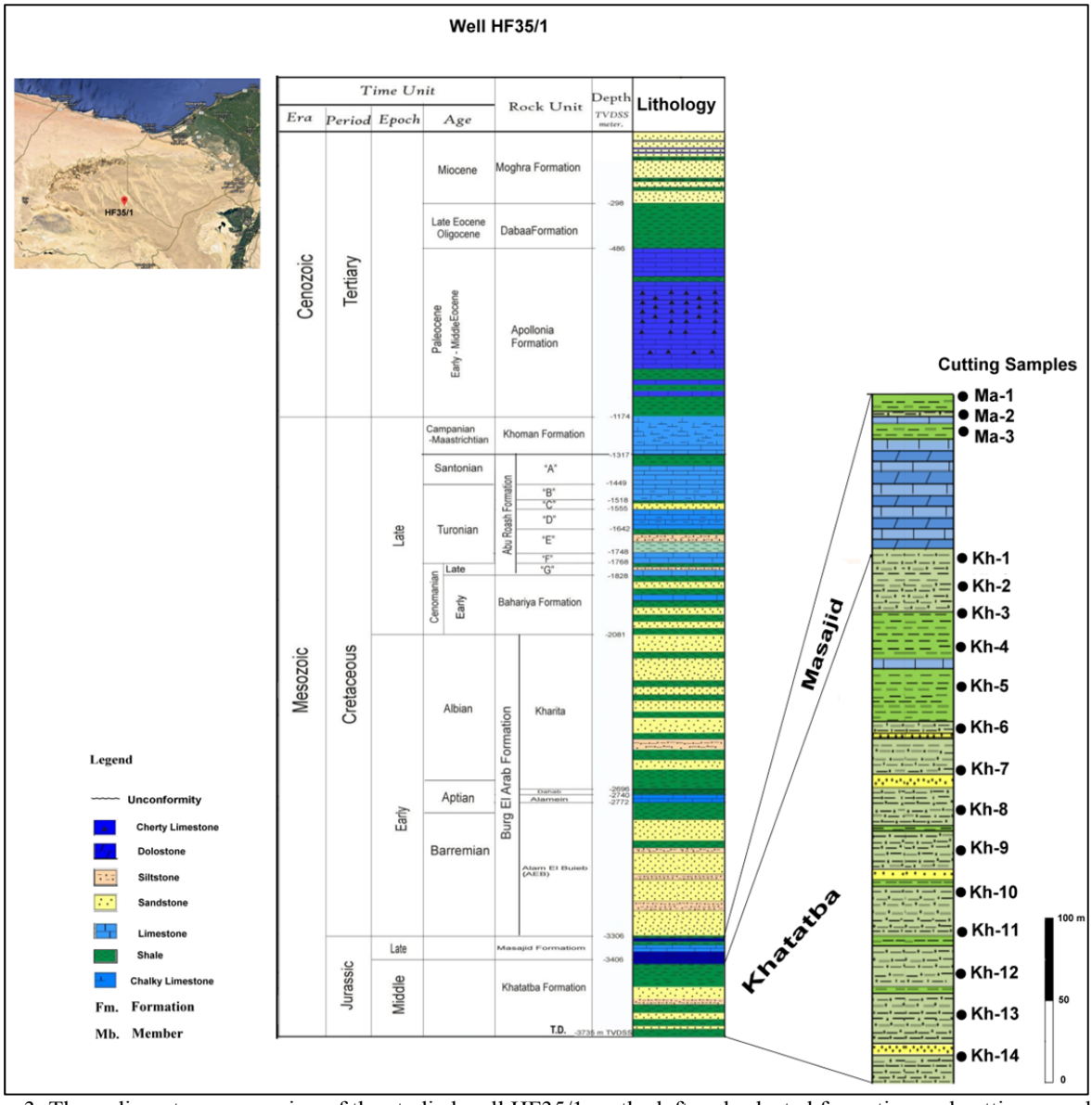

Fig. 3: The sedimentary succession of the studied well HF35/1 on the left and selected formation and cutting samples at the right.

Potential yield PY = S1 + S2 (mg HC/g rock); oxygen index OI = S3 × 100/TOC (mg CO/g TOC); hydrogen index HI = S2 × 100/TOC (mg HC/g rock) S2/S3 (for determining Type of Kerogen; production index PI = S1/S1+S2; oil saturation index OSI = S1 × 100/TOC were the calculated parameters measured during the present study (Peters and Cassa 1994; Hunt 1996; Espitalie et al. 1997; Fowler et al. 2005; Gürgey and Bati 2018).

The Ro is calculated for each sample based on the equation of Jarvie et al. (2001): % Ro= 0.018x Tmax-7.16. Statistical relationships and fit linear regression between the components of depth, and the obtained data of vitrinite reflectance are carried out using Origin-Pro statistical-graphical software version 8.

RESULTS

The measured and calculated parameters from the Rock-Eval analysis of the selected Formations were reported in the Table (1). The obtained results were used for determining the hydrocarbon potential of the Upper and the Middle Jurassic formations (Masajid and Khatatba). Tmax , PI, and calculated Ro values in the studied samples give a viewpoint indication of the degree of maturity of OM. An attempt to predict the immature, mature, and postmature interval within the studied well is also measured using the coefficient of the linear regression between Ro and burial depth.

To interpret the samples without giving an error the each sample contaminated by oil or of overmature is concealed. The Jarvie et al (2001) suggested the oil saturated index OSI= (S1/TOC) x 100 to determine contaminated hydrocarbon samples. From which all samples have the OSI values from 7.14 to 44 that refer to uncontaminated samples. Moreover, by plotting of the S1 against TOC values of the present samples illustrates that all samples are fit below the proposal line of contamination where OSI equal 100 (Fig. 4).

On the other hand, the postmature samples are those samples having Ro higher than 1.35 and Tmx higher than 475^{o}C according to (Peter and Casse1994; Rahmani et al. 2013). The entire samples of the present study have values less than the above-mentioned limits. The measured values of Tmax within the studied formation lay between 454^{o}C and 464^{o}C. The calculated Ro values are within the limits between 1.01 and 1.19. Both values of Tmax and Ro show an increase in its values of younger (Masajid) to older (Khatatba) of the Upper to the Middle Jurassic respectively. The previous parameters show an increase with increasing the burial depth related to the traditional increase of the geothermal gradient in the study area.

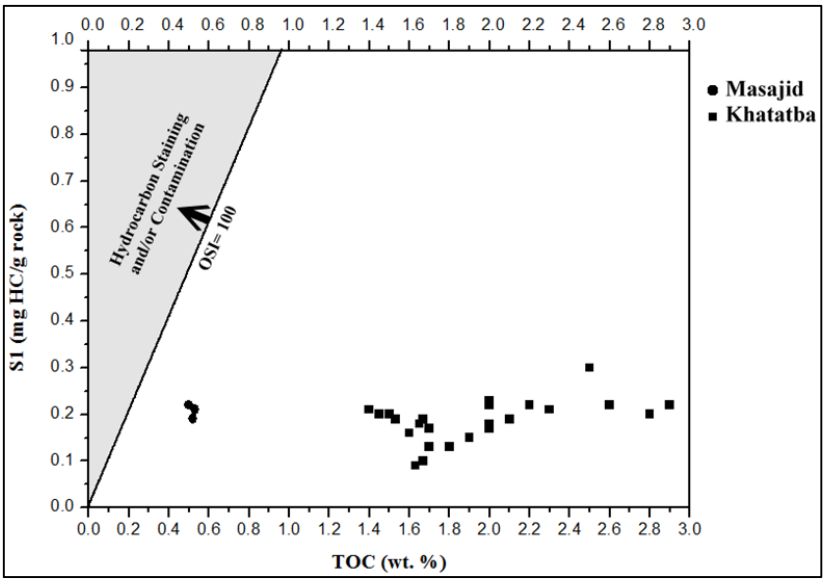

Fig. 4: S1 against TOC diagram of the studied formations Masajid and Khatatba, well HF35/1, Abu Sennan area, W.D. (Jarvie et al., 2001). Note: shadow area representative samples of possible contamination

The quantity of organic richness

The amount of the OM in the sedimentary strata generally refers to the amounts of TOC (wt, %) (Tissot and Welte, 1984). The releasing hydrocarbons by increasing the degree of the thermal maturity is mentioned as the S1, and S2 (Peters and Cassa 1994; Hunt 1996). The TOC values of Masajid are situated in between the poor and fair source rock (Table 1; Fig. 5). The Khatatba show better values of the measured TOC. A plotted 17 samples of the Khatatba lies within the area of good source nearly 71 % of its represented samples (TOC; 1.4-2 wt, %) where the rest samples (29 %) show a very good source of TOC > 2 to 2.9 wt, %. The other parameters of S1 and S2 confirmed that both of the studied formations exhibit low values of S1 (0.09-0.23; average 0.19 mg HC/gm rock) and S2 (0.32-6.02; average 2.26 mg HC/gm rock).

Table 1: TOC, Rock-Eval pyrolysis, and vitrinite reflectance data and indices of Masajid and Khatatba Formations, Well no. HF35/1, Abu Sennan area, north Western Desert.

Formations	Cutting Samples	Drilled Depth (m)	TOC (wt, %)	S1 (mg HC/g rock)	S2 (mg HC/g rock)	S3 (mg CO2/g rock)	T max (^{o}C)	Ro calculated (%)	Production Yeild Py=S1+S2	S2/S3	Hydrogen Index (mg HC/g TOC)	Oxygen Index (mg CO2/g TOC)	Production Index PI=S1/(S1+S2)	Oil Saturation Index OSI=S1x100/TOC
Masajid	Ma-1	3500	0.5	0.22	0.38	0.1	457	1.06	0.6	3.8	76	20	0.37	44
	Ma-2	3512	0.53	0.21	0.32	0.09	454	1.01	0.53	3.56	60.38	16.98	0.4	39.62
	Ma-3	3523	0.52	0.19	0.34	0.11	458	1.08	0.53	3.09	65.38	21.15	0.36	36.54
Khatatba	Kh-1	3600	1.7	0.17	1.28	0.36	460	1.12	1.45	3.56	75.29	21.18	0.12	10
	Kh-2	3612	1.6	0.16	1.23	0.38	462	1.16	1.39	3.24	76.88	23.75	0.11	10
	Kh-3	3623	1.65	0.18	1.25	0.38	459	1.1	1.43	3.29	75.76	23.03	0.12	10.91
	Kh-4	3635	1.7	0.13	1.33	0.43	457	1.06	1.46	3.09	78.23	25.29	0.09	7.65
	Kh-5	3646	1.63	0.09	1.21	0.35	458	1.08	1.3	3.46	74.23	21.47	0.07	5.52
	Kh-6	3658	1.67	0.1	1.09	0.28	459	1.1	1.19	3.89	65.27	16.77	0.08	5.99
	Kh-7	3670	1.8	0.13	1.71	0.45	460	1.12	1.84	3.8	95	25	0.07	7.22
	Kh-8	3681	1.9	0.15	2.28	0.65	458	1.08	2.43	3.51	120	34.21	0.06	7.89
	Kh-9	3693	2	0.17	2.5	0.71	459	1.1	2.67	3.52	125	35.5	0.06	8.5
	Kh-10	3705	2.1	0.19	3.15	0.79	460	1.12	3.34	3.99	150	37.62	0.06	9.05
	Kh-11	3716	2.3	0.21	4.14	1.06	462	1.16	4.35	3.91	180	46.09	0.05	9.13
	Kh-12	3728	2	0.18	3.56	0.94	459	1.1	3.74	3.79	178	47	0.05	9
	Kh-13	3740	1.67	0.19	2.51	0.7	461	1.14	2.7	3.59	150.3	41.92	0.07	11.38
	Kh-14	3751	1.5	0.2	2.7	0.69	460	1.12	2.9	3.91	180	46	0.07	13.33
	Kh-15	3763	1.4	0.21	2.49	0.67	464	1.19	2.7	3.72	177.86	47.86	0.08	15
	Kh-16	3774	1.53	0.19	2.3	0.66	462	1.16	2.49	3.48	150.33	43.14	0.08	12.42
	Kh-17	3786	1.45	0.2	2.1	0.53	462	1.16	2.3	3.96	144.83	36.55	0.09	13.79
	Kh-18	3798	2	0.22	2.5	0.46	464	1.19	2.72	5.43	125	23	0.08	11
	Kh-19	3809	2.5	0.3	3	0.75	462	1.16	3.3	4	120	30	0.09	12
	Kh-20	3821	2.6	0.22	3.51	0.92	462	1.16	3.73	3.82	135	35.38	0.06	8.46
	Kh-21	3832	2.8	0.2	6.02	1.94	463	1.17	6.22	3.1	215	69.28	0.03	7.14
	Kh-22	3844	2.9	0.22	3.63	0.36	461	1.14	3.85	10.08	125.17	12.41	0.06	7.59
	Kh-23	3856	2.2	0.22	2.53	0.63	464	1.19	2.75	4.01	115	28.64	0.08	10
	Kh-24	3867	2	0.23	2	0.22	464	1.19	2.23	9.09	100	11	0.1	11.5

By plotting of the calculated production yield (S1+S2) against the TOCvalues of the studied sedimentary sequence on the diagram of Ghori and Haines (2007) indicate that; the majority samples of the Kareem and the Rudies Formations fit in the area of poor potential; the samples represents the Nukhul, the Darat, and the Esna Shale Formations are located in the fair area, while the 13 samples of the Thebes (87 %) lay in the areas of verygood to excellent potential (Fig. 5).

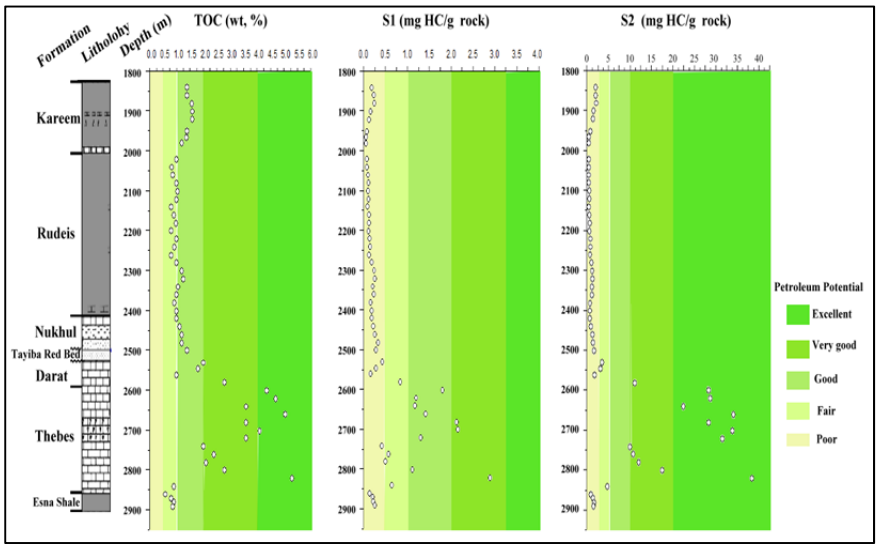

Fig. 4: Plot diagrams of TOC, S1, and S2 versus the burial depth of the studied Formations (Peters and Cassa 1994).

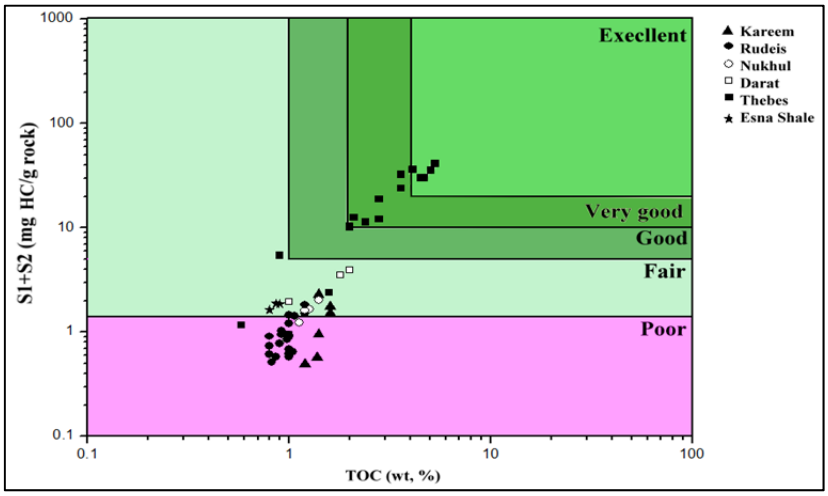

Fig. 5: Plot diagram of Production yield versus TOC of the studied Formations (Ghori and Haines 2007).

Kerogen types

Generally, three and/or four main types of kerogen within the studied sedimentary sequence are distinguished (Figs. 6 & 7). Type I and Type II are the genetic precursor of oil.Type II/III[b] is in between Type II & III of either oil and/or gas prone. Type III of terrestrial plants of dominatinggas-prone and Type IV of inert carbonor oxidized OM (Tissot and Welte, 1984; Waples, 1985; Jacobson, 1991; Van Krevelen, 1993; Peters and Cassa, 1994; Hunt, 1996; Espitalie et al 1997).

The expelled product at the peak maturity is depended essentially on the types of kerogen. The main geochemical parameters identify the kerogen types are HI (mg HC/g TOC) and S2/S3 ratio (Peter and Cassa, 1994). The calculated HI values of the studied samples show that the Kareem, the Rudeis, the Nukhul, and The Esna Shale Formations are belonged to type III kerogen of HI values between 50-200 mg HC/g TOC, with the exception of the Lower Kareem and Upper Rudeis Formation of inert Type-IV Kerogen have of HI values less than 50 mg HC/g TOC. All samples of the Thebes Formationare located within Type I (40 %, of HI > 600 mg HC/g TOC) and Type II (60 % of HI between 300-600 mg HC/g TOC). The S2/S3 ratios of the studied sequence show more reducing types of kerogen than HI values (Fig. 7). The inert Type IV is prolonged from the lower Kareem Formation to cover the entire Rudeis Formation of S2/S3 ratio < 1. Type III is characterized the Upper Kareem, The Nukhul, The Darat, and The Esna Shale Formations of S2/S3 ratio range from 1 to 5. The Thebes Formation displays three different types (Type II, 27%; Type II/III, 40 %, and Type III, 33 %) of S2/S3 ratios range between 10-15, 5-10, and 1-5 in respect order (Fig. 7).

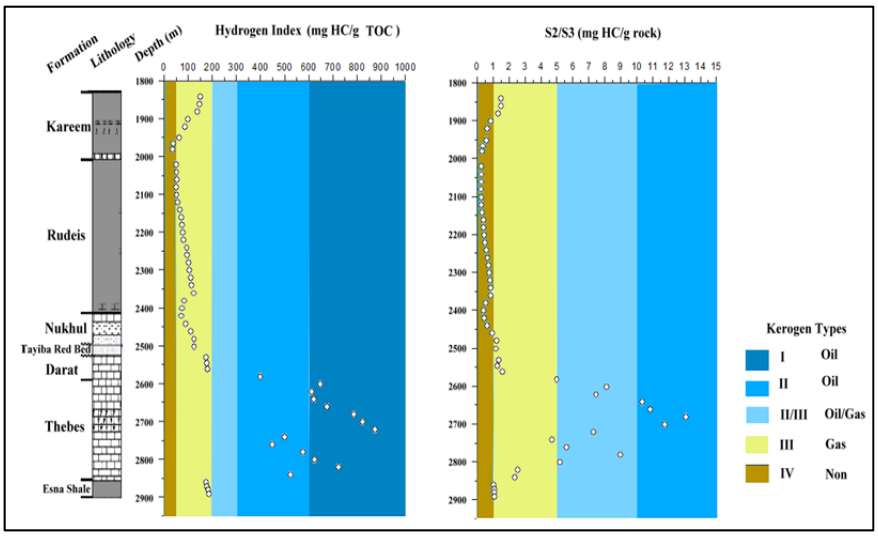

Fig. 6: Kerogen types diagram of the studied Formations based on Peter and Cassa (1994).

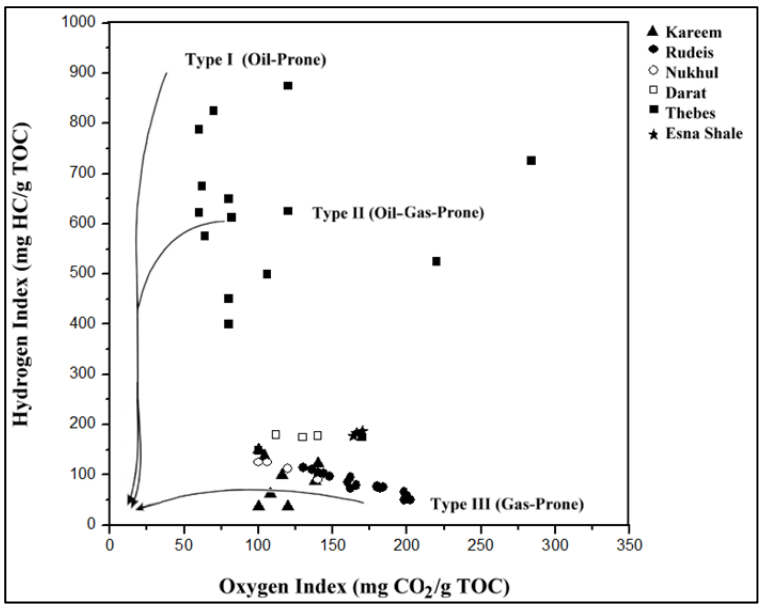

Fig. 7: Plot diagram of HI versus OI diagram of the studied Formations (van Krevelen 1993).

By the plotting of the studied samples on HI versus OI diagram established by Van Krevelen (1993) (Fig. 8). The samples of study Formations of the Kareem, the Rudeis, the Nukhul, the Darat, and the Esna Shale reveal a Type III, with a little bit of Type IV of three samples belong Kareem Formation. On the other hand samples of the Thebes Formation are situated within the areas of Type I and Type II of oil and oil/gas-prone respectively.

Maturity

The rate of the decomposition and alteration of OMto produce oil, wet gas, and finally, dry gas with the increasing temperature, depth, pressures, and time is called maturity (van Krevelen, 1993). Other important factors affect the maturity is the quality and quantity of OM encompass the sedimentary strata (Tissot and Welte, 1984). The measure of the degree of thermal maturity of the studied sedimentary sequence is determined by the Rock-Eval Tmax, PI, and by the measurements of R_O(Peters and Cassa, 1994; Taylor et al., 1998).

The measured Tmax for the whole studied sequence ranges from 419^{o}C for younger Kareem Formation to reach its maximum value of 430^{o}C for the oldest Esna Shale Formation. The PI values of the whole formation show the generative potential of low values immature (37 %; PI < 1) to dominate early mature of the majority of samples of 73 % of 1-0.2 PI (Table 1).

Vitrinite reflectance data assemble to the Tmax values initiates with the low values (0.32 %) for younger strata and reach progressively to its maximum values (0.62 %) for the oldest Esna Shale Formation in the studied sequence.

The relationship between vitrinite reflectance against depth observes that the depth of 2500m appears to separate the low-rank gradient of the Kareem, the Rudeis, and the Nukhul Formations from the high-rank gradient of the Darat, the Thebes, and the EsnaShale Formations. The measurements of vitrinite reflectance data after preceding that depth increase six times than its values in the upper sequence at the similar depth interval (Fig. 9A). An estimation of the thickness of eroded sediments in term of maximum depth of burial of the studied sequence is established according to Suggate (1998). The profile of the Roagainst the depth (Fig. 8A) is plotted on the standard diagram with taking into account the slope of low-rank gradient and curve of bending and the slope of the high-rank gradients. The fittest linesmatching with the proper profile perfectly match with the line of the geothermal gradient of 28^{o} C/km. The subtraction distance of the upper-end line of zero depth to the standard profile of Suggate is used to presume the maximum burial depth of the selected sequence of approximately 2090m (Fig. 8B).

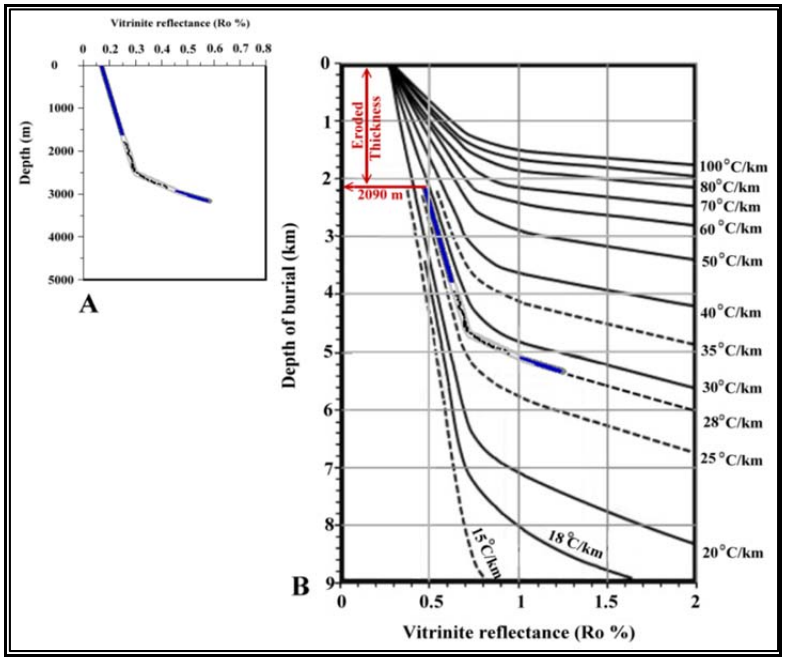

Fig. 8: Plot diagram of vitrinite reflectance versus the burial depth of the studied Formations on the left, and the same diagram was plotted on the standard Suggate diagram on the right (Suggate 1998).

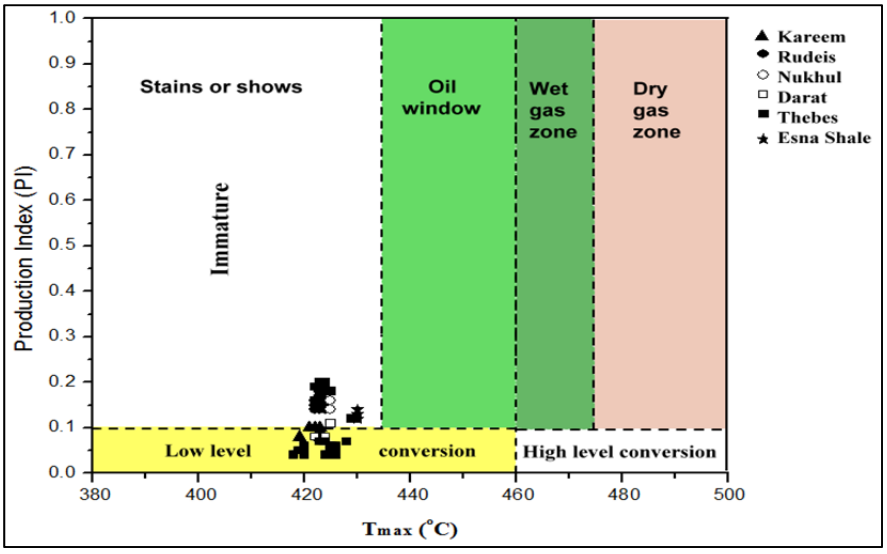

Fig. 9: Plot diagram of production Index versus Tmax of the studied Formations (Ghori and Hains 2007).

Thermal maturity is also illustrated by the plotting of the studied samples on the thermal maturity diagrams of both Chori & Haines (2007) of the Tmax against PI and Tmax versus HI according to Koerverdon et al. (2011)(Figs. 9&10). The half of samples lay within the area of low-level conversion and half within stains or a show on the immature stage of maturation (Fig. 9). Koeverdon diagram shows also the premiere of the Thebes Formation of Type I, II, and II/III than other studied Formations of Type III, IV-III, and IV. Although the entire formation site in the immature zone with the exception of marginally mature in case of Esna Shale samples (Fig. 10).

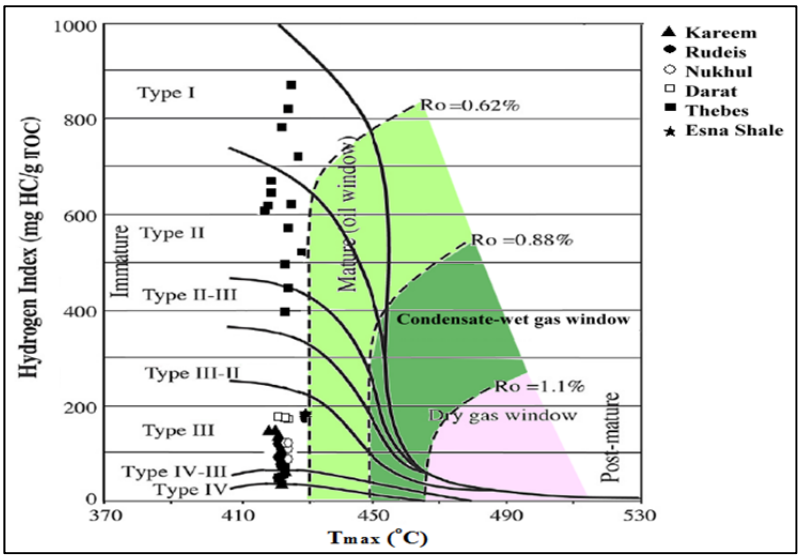

Fig. 10: Plot diagram of Hydrogen Index versus Tmax diagram of the studied Formations (Koeverdon et al. 2011).

Potential sea level sysles and detecting oil window interval

The relative hydrocarbon potential RHP (=S1+S2/TOC) parameter derives from the Rock-Eval can be used as proxies for sea level oscillation (Fang et al., 1993, Gürgey and Bati, 2018). The present studies of the studied sequence show two major cycles (Fig. 11). The lower cycle is characterized by RHP > 2 in which the highest sea level is recorded (9.11 RHP) at the middle part of the Thebes Formation.In contrast, the upper cycle is distinguished by RHP < 2 in which the lowest sea level is recorded(0.41 RHP) within the Lower part of the Kareem Formation (Table 1; Fig. 11).

Within these major cycles, a minor sea level oscillationis pointed out, of four oscillations related to the lower major cycle and of five oscillations in the upper major cycle of the relative dominance of anoxic-oxic conditions (Fig. 11).

The dogleg shaped of the measured vitrinite reflectance versus the burial depth of the selected sequence within the EE85-1A well give us the ability to separate each zone of data and applied statistical studies to give a linear relationship concerns each part (Fig. 12). By applying a coefficient of the linear regression on the upper sequence (the Kareem, the Rudeis, and the Nukhul Formation) above the depth of 2500 m shows that the vitrinite reflectance increase slowly by trigger increasing in depth (n= 32, r=0.94, and Sd= 0.006). Dissimilarity, the lower part of the Darat, the Thebes, and the Esna Shale Formation displays a rapid increase in vitrinite reflectance with little increase in depth (n=22, r=0.98, and Sd=0.01). By drawing lines representing a different maturation zone based on vitrinite reflectance crossing the extended dot lining that was drawn according to the statistical regression relationship of the studied samples, the active oil zones are recognized between 2890 m and 4450 m.

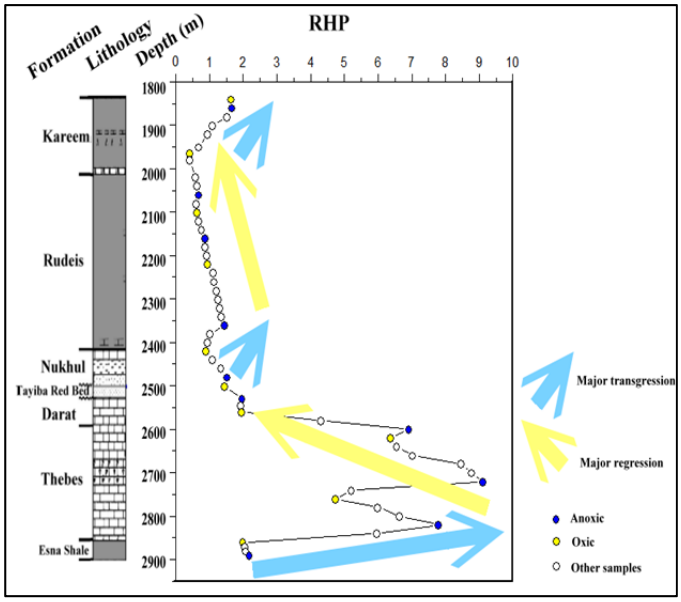

Fig. 11: Transgression-regression mega-cycles of the studied Formations based on a RHP parameter (Fang et al. 1993).

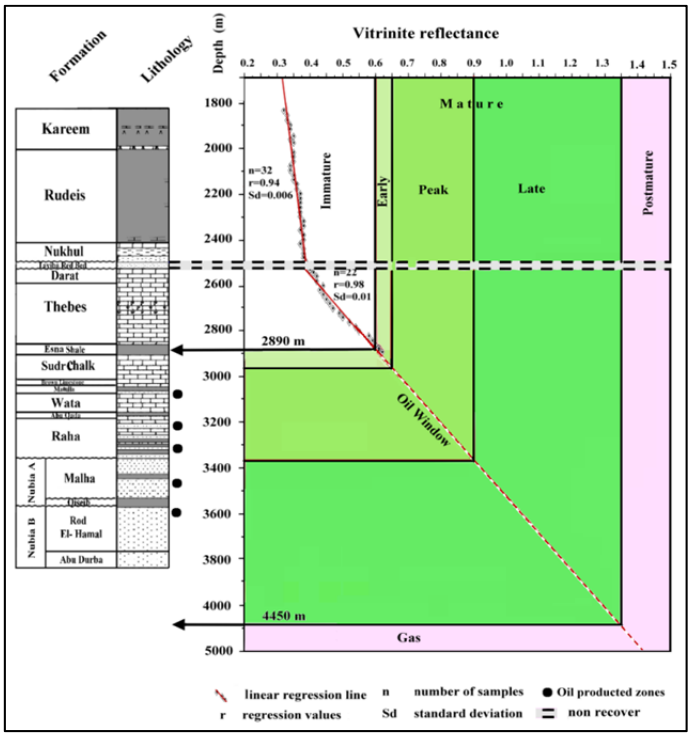

Fig. 12: Predicted thermal maturity levels of the studied Formation (Peters and Cassa 1994).

DISCUSSION AND CONCLUSION

The selected sedimentary Formations from the well EE85-1A is an important sequence in the Suez Gulf. It includes two mega-sequences from the main fives mega-sequences throughout the Gulf history (Bosworth et al., 1998; Peijs et al, 2012). The third mega-sequence of Pijis et al. (2012) initiated from The Duwi Formation until thevDarat Formation synchronousonset of the Syrian-Arc to the clysmic-Rift tectonics. The fourth mega-sequence corresponds to the Nukhul, the Rudeis, and the Kareem Formation of the Rift-infill contemporary the proper clysmic rift to the onset of the Dead Sea tectonics (Patton, 1994; Moustafa and Khalil, 1995).

The above-mentioned mega-sequencesare coinciding with the obtained results of the present two mega-cyclesof sea level illustrated by the geochemical parameter of RHP (Fig. 11).

The TOC contents of the studied Formation according to the classification of Peters and Casss (1994) show three categories of petroleum potential (Fig. 4). The first is fair related to both the Rudeis and the Esna Shale Formations. The second is good for the Kareem, the Nukhul, and the Darat Formations. The Thebes Formation is a very good to excellent. Generally, the high values of TOC can give conformity of either good preservation or high biota and/or flora productivity (Jasper et al., 2010).

However, the TOC cannot be used as the sole parameter to interpret the OM quantitative due to its contents may be coming from (organic) oxygen, hydrogen, nitrogen, sulfur, etc. (El Atfy et al., 2014). Furthermore, the OM may be subjected to reworking, oxidation or reach to a high post-mature level where exhibit low level of petroleum to be extracted.

So that, both amounts of S1 and S2 are almost used to confirm the petroleum potentiality in combined with the previous TOC contents. The amounts of hydrocarbon release at 300^{o} C of the pyrolysis (S1) and those came from cracking of kerogen at ≈ 600^{o} C (S2) denote all sedimentary Formations are of poor potential with the exception of the Thebes Formation of the majority good to excellent potential (Fig. 4).

Additionally, plotted the obtained data of the studied Formations on Py versus TOC diagram established by Ghori and Haines (2007) demonstrate that the petroleum potential of the all Formations within poor to fair zones, whereas, The Thebes Formation displays dominance (80 %) of very good to excellent potential (Fig. 5).

Quality is expressed in the present study by HI and S2/S3 ratio (Peter and Cassa, 1994). The change in the kerogen type can also give a good idea in term of transgression- regression assessments

(Habib and Miller, 1989). Omara and Hoyanagi (2004) reported that the transgressive sea suggested by high amounts of HI and low amounts of terrestrial OM (Kerogen III) and increase in aquatic and marine OM of Type I and II. Hart et al. (1994) stated that the increase in the percentages of the Type IV and III in a sedimentary sequence is attributed to the deposition close to the shoreline of dominant regression.

As to plot of study samples on figure seven, according to Peter and Cassa (1994) show the majority of Type IV and III (inert and gas-prone) in all sedimentary Formation excluding the Thebes Formation of type II and I (oil-prone).

Moreover, the values of the S2/S3 ratio of the studied sequence show that the type IV is prevalent in both the lower part of the Kareem Formation and the entire of the Rudeis Formation samples (Fig. 6). The latter observation can point toward either reworking of OM or oxidation by dropping of sea level toward the lower part of the Kareem Formation and deposition of evaporates (anhydrite minerals) that commonly precipitate by decreasing the volume of seawater to reach 70% water loss in comparison to its original volume, that associate exactly by considerable fall of the sea level (Einsele, 1992). Type III is the dominance in the upper Kareem, the Nukhul, the Darat, and the Esna Shale Formations. Again, based on S2/3 ratio the Thebes Formation is the prime quality one in the studied sequence comprises of prevailing Types II and II/III (Fig. 6).

Kerogen type diagram of van-Krevelin (1993) is also used to detect the types of the studied OM-bearing the sedimentary Formations. In which, all studied Formation occupies the area of Type III and three samples (K6, K7, and K8) of the lower Kareemoccupy the type IV pathway (Table 1), while the types II and I belong only to the Thebes Formation (Fig. 7).

The aforementioned result reveals that the Thebes Formation is the only of the studied sequence is capable to be the effective source rock of both high TOC and very-good quality of Kerogen Types I and II if it is subjected to the appropriate thermal maturity level.

Unfortunately, the obtained results of the thermal maturity parameters of Tmax, Ro, and PI in the present study show all the studied Formations are immature or marginally early mature in case of the deepest burial depth of The Esna Shale Formation (Figs, 9-10, 12).

The most important conclusion that the promising Thebes Formation cannot be an effective source rock except if it is buried enough to proceed the active, measuredoil-window zone suggested by the present study intervals between 2890 and 4450 m under a geothermal gradient of 28^{o}C/km. Maky et al. (2010) mentioned that the Thebes Formation is one of three considers a very good source rock within the central Gulf area. In his study, the Thebes Formation was founded at great depth intervals between 3716 m and 3945 m in the well WFA-1 and between 3109 m and 3429 m in the well GS 197-2. From the above-mentioned wells, the Thebes Formation reaches to burial depths enough to subject an appropriate thermal maturity level that suggested in between 2850 m and 4450 m depth of the oil-window potentials in the present study (Fig. 12).

Generally, in the subsurface wells, the relationship between the Ro and depth are characterized by two linear gradient segments connected together by a bending segment. Suggate (1998) stated that the Ro in the lower gradient segment increases more rapidly than within the upper gradient segments.

Consequently, by drawing a dots relationship between the Ro and the depth of the present samples, a two trend of the approximately linear relationship is present above and below a depth of 2500 m (Fig. 8A). To illustrate the upper and lower linear gradient a statistical regression line is measured by software of Origin Pro (Fig. 12), in which the rate of increasing Ro in the lower linear gradient is six times more than the rate of its increase in the upper linear gradient (Fig. 12). The lower linear gradient is used in the present study by a combination of maturity values according to Peter and Cass (1994) to predict the active mature oil-window interface.It is suggested within the depths of 2890 m and 4450 m, after that depth a postmature is present. The fifth produced oil reservoirs from the present well are situated within the present study peak and late mature horizons (Fig. 12).

According to Suggate the values of Ro of the present day well are not coinciding with the nowadays measured depths. So that, Suggate (1998) draw a standard diagram to detecting the ancient depth before any missing of strata occur either by erosion from the surface of the studied sequence or by an unconformities in between or within the different studied Formations (Fig. 8B). By transfer, the previous relation between Ro and Depth (Fig. 8A) on the standard diagram of Suggate (Fig. 8B), two

important data are revealing. Firstly, the studied sedimentary sequence is located within the geothermal gradient of 28^{o}C/km. Secondly; the missing of strata reaches 2090 m, or by another meaning, the ancient burial depths for Ro values of the studied sequence must be higher than the present day depths by adding 2090 m thickness.

The sea level cycles based on geochemical parameter RHP and HI in the present study have inappropriate with the fact of invasion of the sea over Egypt reached its fairly deep marine during the deposition of Thebes Formation and sea retreat again at the end of Late Eocene (Issawiet al., 1999). The sharp cycle (lower cycle) of the pre-rift strata were started by a high transgression from the end of the Esna Shale Formation to reach its threshold during the middle of the Thebes Formation of prevailing anoxic condition (Fang et al., 1993). After that, the sea retreats again by sharp regression until the end of the Darat Formation (Fig. 11). The second cycle (upper cycle) is a mild one, was started by transgression during the syn-Rift deposition of the Nukhul Formation, then sea retreats again throughout the Rudeis Formation till the Lower Kareem Formation, then the level of sea flooded again during the deposition of the Upper Kareem Formation.

It worth to mention from the present study there is a vital relationship between the type of kerogen and transgression-regression sea level change (Figs. 6 & 11). The maximum transgression characterized by dominating Type I and II of the Thebes Formation mainly of marine origin and oil-prone potential, whereas maximum regression characterized by the dominators of Types IV and III of terrestrial origin and inert to gas-prone potential. The maximum oxic condition in the present sea level cycles associated with the presence of anhydrite streaks minerals that precipitate chemically by a fatal drop of sea level at the lower part of the Kareem Formation.

ACKNOWLEDGMENTS

The authors give kindly thanks to the (EGPC) Egyptian General Petroleum Company for providing us the cutting samples, the stratigraphic sequence, and well-log chart for the studied well to accomplish this study. Great thanks also to Dr Ivana Sykorova in the IRSM of the Czech Republic for her kindly measurments of the Ro of the studied samples.

REFERENCES

Abdel Zaher, M.; Saibi, H., ElNouby M.; Ghamry, E.; Ehara, S.(2011): A preliminary regional geothermal assessment of the Gulf of Suez, Egypt. J. Afr. Earth Sci. 60(3), 117-132

Afifi, A. S.; Moustafa, A. R.;Helmy, H. M.(2016): Fault block rotation and footwall erosion in the southern Suez rift: Implications for hydrocarbon exploration. Marine & Petrol. Geol., 76, 377-396.

Ali, R. and Khairy, A. (1996): EGPC 13th Petroleum Conf., Exploration, Cairo, Egypt 2, 396-409.

Alsharhan, A.S. (2003): Petroleum geology and potential hydrocarbon plays in the Gulf of Suez rift basin, Egypt AAPG, Bull. 87, 143-180.

Alsharhan, A. S.; Salah, M. G. (1995): Geology and hydrocarbon habitat in rift setting: northern and central Gulf of Suez, Egypt. Bulletin of Canadian Petroleum Geology 43(2), 156–176.

Atia, M. H.; Ahmed, A.M.; and Korrat, I.(2015): Thermal Maturation Simulation and Hydrocarbon Generation of the Turonian Wata Formation in Ras Budran Oil Field, Gulf Of Suez, Egypt. Rev. J. Environ. Sci, 44(1), 57-92.

Abu Al-Atta, M.; Issa, G. I.; Ahmed M. A.; Afife, M. M. (2014): Source rock evaluation and organic geochemistry of Belayim Marine Oil Field, Gulf of Suez, Egypt. Egypt. J. Petrol., 23, 285–302

Barker, C. E. (1996): A comparison of vitrinite reflectance measurements made of wholerock and dispersed organic matter concentrate mounts. Organic Geochem. 24, 251-256.

Bosworth, W.; Crevello, P.; Winn Jr. R. D.; Steinmetz, J. (1998): Structure, sedimentation, and basin dynamics during rifting of the Gulf of Suez and north-western Red Sea. In: Purser, B. H.; Bosence, D. W. J. (Eds.), Sedimentation and Tectonicsin Rift Basins: Red Sea Gulf of Aden. Chapman Hall, London, 77-96.

Boukhary, M.; Abd El Naby, A.; Faris, M.; Morsi, A. (2012): Plankton stratigraphy of the Early and Middle Miocene Kareem and Rudeis Formations in the central part of the Gulf of Suez, Egypt. Hist. Biol 24, 49-62.

Chowdhary, L. R. S. and Taha, M. A. (1987): Geology and habitat of oil in Ras Budran field, Gulf of Suez. AAPG Bull. 71, 1274-1293.

Chowdhary, L. R.; Shaheen, S.; Naggar, A. A. (1986): EGPC 8th Exploration Conference, Cairo, Egypt, pp. 308-321.

Darwish, M. and El Araby (1993): Petrography and diagenetic aspects of some siliclastic hydrocarbon reservoir in relation to the rifting of the Gulf of Suez, Egypt. Geol. Soc. Egypt, Spec. Publ. 1, 155-187.

Darwish, M.; El Barkooky, N. A.; Tewfik, N.; Hellem, T.; Amundsen, H.(1998): Early Rift facies and tectonics in the Gulf of Suez, Egypt "Nukhul Block" as a case study: AAPG BULL. Hedberg Conference.

Dolson, C. J.; Shaan, V. M.; Matbouly, S.; Harwood, C.; Rashed, R.; Hammouda, H.(2001): The Petroleum Potential of Egypt. In: Downey, W. M.; Threet, C. J.; Morgan, A. W. (Eds.), Petroleum proviences of the twenty-first century. AAPG BULL. Tulsa, Oklahoma. 453-482.

EGPC (Egyptian General Petroleum Corporation) (1996): Gulf of Suez Oil Fields, A Comprehensive Overview. Cairo, Egypt.

Einsele, G. (1992): Sedimentary Basins: Evolution, Facies and Sediment Budget. Springer-Verlag Berlin Heidelberg , Germany.

El Atfy H.; Brocke, R.; Uhl, D.; Ghassal, B.; Stock, A. T.; Littke, R. (2014):Source rock potential and paleoenvironment of the Miocene Rudeis and Kareem formations, Gulf of Suez, Egypt: An integrated palynofacies and organic geochemical approach. Inter. J. coal geol., 131, 326-343.

El Diasty, W. S.; El Beialy, S. Y.; Abo Ghonaim, A. A.; Mostafa, A. R.; El-Atfy H., (2014): Palynology, palynofacies and petroleum potential of the Upper Cretaceous-Eocene Matulla, Brown Limestone and Thebes formations, Belayim oilfields, central Gulf of Suez, Egypt. J. Afr. Earth Sci., 95, 155-167.

El-Khadragy, A. A.; Shazly, T. F.; Ramadan, M.; El-Sawy M. Z. (2017): Petrophysical investigations to both Rudeis and Kareem formations, Ras Ghara oil field, Gulf of Suez, Egypt. Egypt. J. Petrol., 26, 269-277

El Nady, M. M. (2006): The hydrocarbon potential of Miocene source rocks for oil generation in the South Gulf of Suez. Egypt. J. Pet. Sci. Tech. 24, 309-361.

El Nady, M. M. and Mohamed N. S.(2016):Source rock evaluation for hydrocarbon generation in Halal oilfield, southern Gulf of Suez, Egypt. Egyptian Journal of Petroleum 25, 383-389,

El Nady, M. M.; Harb, F. M.; Mohamed, N. S. (2016): Geochemical characteristics of organic matter from Rudeis and Kareem source rocks, Ras Budran oilfield, central Gulf of Suez, Egypt. Energy sources, Part A: Recovery, utilization, and environmental effect 38(22), 3273-3282

Espitalie, J. M.; Laporte, J. L.; Madec, M.; Marquis, F.; Laplot, P.; Paulet, J.; Boutefeu, A.(1997): Rapid method for source rock characterization, and for determination of their petroleum potential and degree of evolution. Revue de l'Institut Francais du Petrole et Annales des Combustibles Liquids 32, 23-24.

Fang, H.; Jianyu, C.; Yongchuan, S.; Yaozong, L. (1993) Application of organic facies studies to sedimentary basin analysis: a case study from the Yitong Graben, China. Org Geochem. 20, 27-47.

Fowler, M.; Snowdonand, L.; Stasiuk, V. (2005): Applying petroleum geochemistry to hydrocarbon exploration and exploitation, AAPG Short Course Notes, June 18-19, 2005, Calgary, Alberta..

Ghori, K. A. R. and Haines, P.W. (2007): Paleozoic Petroleum Systems of the Canning Basin, Western Australia: A review. Search and Discovery Article #10120.

Gürgey, K. and Bati, Z. (2018): Palynological and petroleum geochemical assessment of the Lower Oligocene Mezardere Formation, Thrace Basin, NW Turkey. Turkish J. Earth Sci., 27, 349-383.

Henaish, A.(2018): Fault-related domes: Insights from sedimentary outcrops at the northern tip of the Gulf of Suez rift, Egypt. Marine and Petroleum Geology, 91, 202-210.

Hunt, J. M. (1996): Petroleum Geochemistry and Geology 2nd Eds., W. H. Freeman and Company.

ISO 7404/5(2009): Methods for the petrographic analysis of bituminous coal and anthracite. Part 5: Method of determining microscopically the reflectance of vitrinite. International Organization for Standardization. Geneva. Switzerland

Issawi, B.; El Hinnawi, M.; Francis, M.; Mazhar, A. (1999): The Phanerozoic Geology of Egypt: a Geodynamic Approach, vol. 76. Egyptian Geol. Survey Spec Publ. 1-462

Jasper, K.; Hartkopf-Fröder, C.; Flajs, G.; Littke, R. (2010): Evolution of Pennsylvanian (Late Carboniferous) peat swamps of the Ruhr Basin, Germany: comparison of palynological, coal petrographical and organic geochemical data. Inter. J. Coal Geol., 162, 346-365.

Jarvie, D. M.; Morelos, A.; Han, Z. (2001): Detection of pay zones and pay quality. Gulf of Mexico: application of geochemical techniques. Gulf Coast Assoc. Geol. Soc. Transactions. 51, 151-160

Khairy, A. and Swidan, N. (1992): EGPC 11th Exploration and Production Conference, Cairo, Egypt, Exploration. 396-409.

Koeverdon, J. H. V.; Karlsen, D. A.; Backer-Owe (2011): Carboniferous non-marinesource rocks from Spitsbergen and Bajornoya: comparison with westernArctic. J. Petrol. Geol. 34 (1), 53-66.

Lüning, S.(2005): North African Phanerozoic, In:Selly, R. C., Cocks, L. R. M., Plume I. R. (Eds), Encyclopedia of Geology, Elsevier Academic Press, 12-26.

Maky, A. F.; Mousa, A. S.; Mohamad, N. I. (2010): Source rock and paleoenvironmental evaluation of some pre-rift rock units at the central part of the Gulf of Suez, Egypt. J. App. Sci. Res., 6(2), 511-528.

Moustafa, A. R.(2002): Controls on the geometry of transfer zones in the Suez rift and northwest Red Sea: Implications for the structural geometry of rift systems. AAPG, Bull 86, 979-1002.

Moustafa, A. R.; Khalil, M. H. (1995): Superposed deformation in the northern Suez rift, Egypt: relevance to hydrocarbon exploration. J. Petrol. Geol., 18, 245-266.

Nabawy, B. S. and El Sharawy, M. S. (2018): Reservoir assessment and quality discrimination of Kareem Formation using integrated petrophysical data, Southern Gulf of Suez, Egypt. Marine and Petroleum Geology 93, 230-246.

Patton, T. L.; Moustafa, A. R.; Nelson, A. R.; Abdine, A. S. (1994): Tectonic evolution and structural settings of the Gulf of Suez rift. In: M. S. (Eds.) Interior rift basins. London. AAPG BULL. Memoir (59), 9-56

Peijs, J. A. M. M.; Bevan, T. G.; Piombino, J. T. (2012): The Gulf of Suez rift basin, In: Phanerozoic Rift Systems and Sedimentary Basins, Elsevier, pp.165-194.

Peters, K. E., and Cassa, M. R. (1994): Applied source rock geochemistry. In: Magoonand, L. B., Dow, W. G., (Eds.). The petroleum system from source to trap. AAPG. 93-120.

Rahman, S. A. and Zahran, I. (1986): Contribution of V.S.P. in understanding the structural pattern in Ras Budran area, Gulf of Suez, Egypt. EGPC 8th Exploration Conference, Cairo, Egypt 2, 417-433.

Rahmani, O.; Aali, J.; Junin, R.; Mohseni, H.; Padmanabhan, E.; Azdarpour, A.; Zarza, S.; Moayyed, M.; Ghazanfari, P. (2013): The origin of oil in the Cretaceous succession from the South Pars Oil Layer of the Persian Gulf. Inter. J. Earth Sci., (Geol Rundsch) 102, 1337-1355

Salah, M. G. (1992): Geochemical Evaluation of the Southern Sector of the Gulf of Suez, 11th EGPC Explor. Semin., Egypt, 383-395.

Schumacher, B. A.(2002): Methods for the determination of total organic carbon (TOC) in soils and sediments. ERASC, Office of Research and Development US. Environ. Protection Agency. 1-25.

Shahin, A. N. (1988): Oil window in the Gulf of Suez. Abs., AAPG, BULL. 72, 1024-1025.

Suggate, P. R. (1998): Relations between depth of burial, vitrinite reflectance and geothermal gradient. J. Petrol. Geol., 21(1), 5-32.

Taylor, G. H.; Teichmuller, M.; Davis, A.; Diessel, C. F. K.; Littke, R.; Robert, P.(1998): Organic petrology, Berlin, Gebruder Borntraeger.

Tissot, B. P. and Welte, D. H. (1984): Petroleum Formation and Occurrence, 2nd ed. Springer, Berlin.

Younes, M. A.(2001):Application of biomarkers and stable carbon isotopes to assess the depositional environment of source rocks and the maturation of crude oils, East Zeit Field, southern Gulf of Suez, Egypt. Petroleum Sci. and Tech., 19, 1039-1061.

Van Krevelen, D. (1993): Coal: Typology, Chemistry, Physics and Constitution. Coal Science and Technology Series3.Elsevier, Amsterdam.

Waples, D. W. (1985): Geochemistry in petroleum exploration. International Human Resources and Development Corporation, Boston.

Zahra, H. S. and Nakhla, A. M. (2015): Deducing the subsurface geological conditions and structural framework of the NE Gulf of Suez area, using 2-D and 3-D seismic data. NRIAG Journal of Astronomy and Geophysics 4, 64-85.

دراسات جيوكميائية عضوية على التتابعات الترسيبية من عصر الباليوسين الى عصر المايوسين الاوسط ببئر EE85-1 ، منطقة رأس بدران، خليج السويس، مصر.

خالد أحمد مصطفى خالد و نادر أحمد أحمد إدريس

قسم الجيولوجيا – كلية العلوم – جامعة حلوان

الخلاصة

تقع منطقة رأس بدران فى الجزء الاوسطى الشرقى بالمياة الضحلة بخليج السويس. تم اختيار التتابع الرسوبى من عصر الباليوسين الى أسفل عصر المايوسين الاوسط لتقييمه ودراسته فى البئر EE85-1 بمنطقة رأس بدران. الدراسات الجيوكميائية بواسطة الروك ايفال والمعامل الفيترينى تم تطبيقها لتقييم المكونات الترسيبية المدروسة من وجهة نظر النظام البترولى . منها تم تجميع عدد اربعة وخمسون عينة حفر تمثل ستة مكونات صخرية هي مكون أسنا، مكون تيبيس ، مكون دارات ، مكون نخل، مكون روديس، ومكون كريم تشملهم العصور المختارة .

اظهرت الدراسة الحالية ثلاث فئات مختلفة لصخور المصدر على حسب الجهد البترولى. الفئة الاولى وتشمل مكون تيبيس وهو تم تصنيفه على انه صخر مصدر من النوع الجيد جدا الى الممتاز اعتمادا على ما يحيويه من الكربون العضوى والناتج العضوى وهما ٣.٢ و ٢٢.١ بالترتيب . الفئة الثانية ذات الجهد المنخفض وتشمل مكونات نخل و دارات وإسنا وتحوى كربون عضوى ١.٢٣-١.٦-٠.٨٥وناتج عضوى ١.٦٧-٣.١٣- ١.٨ بالترتيب. الفئة الثاثة تم تصنيفها على انها صخر مصدر فقير وتشمل كلا المكونين كريم وروديس بنسبة كربون عضوى ١.٤-٠.٩٥ وناتج عضوى ١.٥-٠.٠٩٢

أظهرت الدراسة أن نوع الكيروجين بالمكونات المدروسة يشمل النوع واحد واثنين الذى ينتج الزيت والغاز بمكون تيبيس والذى يحتوى على HI أكثر من ٤٠٠ ونسبة S2/S3 تصل قيمتها الى ٦.٩٧ بالمتوسط . الدراسة الحالية اكدت ان مكون تيبيس هو صخر مصدر ذو تاثير قوى بخليج السويس إذا تم دفنه لعمق أكثر للوصول الى العمق المناسب لنطاق نافذة البترول . اظهرت المكونات الأخرى المدروسة انها مكونات ضعيفة الى فقيرة وإذا أنتجت فإنها لن تنتج غير الغاز لما تحويه من كيروجين من النوع الثالث والرابع بقيمة HI لاتتعدى ٢٠٠ ونسبة S2/S3 لا تتجاوز ٢ .

بدراسة المعامل الفيترينى للمكونات المدروسة أتضح أن كل المكونات الرسوبية المدروسة غير ناضجة أو تقع على حافة النضوج حيث انها لم تتجاوز ٠.٠٦٢. الدراسة الحالية اظهرت نطاقين كبيرين لتذبذب مستوى سطح البحر اعتمادا على RHP . تم تحديد أقصى ارتفاع لسطح البحر بالجزء الاوسط من مكون تيبيس والذى تزامن مع أقصى تقدم لسطح البحر اقليميا ، والذى أدى بدورة الى ظروف مواتية لاثراء مكون تيبيس بالمواد العضوية البحرية اثناء الترسيب.